3 Results

3.1 Search for a GPI anchored protease that is involved in mechanotransduction

Vallet and colleagues reported that a serine protease that they named CAP-1 (channel activating protease) activates the epithelial sodium channel ENaC (Vallet et al., 1997). Sequence analysis revealed that CAP-1 is probably a protein that is linked to the plasma membrane via a GPI-anchor (glycosylphosphatidylinositol-anchor). ENaC is related to the mechanotransduction channel BNC1, leading us to hypothesize that a CAP-1 like protease may interact and modulate the activity of BNC1 and therefore influence sensory mechanotransduction. In order to test this hypothesis Gary Lewin examined the effect of PIPLC (phosphytidylinositol-specific phopholipase), an enzyme that cleaves GPI-anchors, on mechanotransduction. When he treated the skin-nerve preparation with PIPLC, low threshold mechanoreceptors were severely impaired compared to control receptors. These studies showed for the first time, that a GPI-anchored protein is involved in mechanotransduction. I have attempted to purify this protein using biochemical methods.

So far, there has not been any description of a GPI-anchored protease in the sensory system. Therefore I first wanted to show that GPI-anchored serine proteases are expressed in the axons of DRG neurons. For this purpose, I dissected out both sciatic nerve from mice and treated one with the enzyme PIPLC and the other with buffer as a control. The supernatant, that should contain released GPI-anchored proteins, was tested for protease activity using a protease gel.

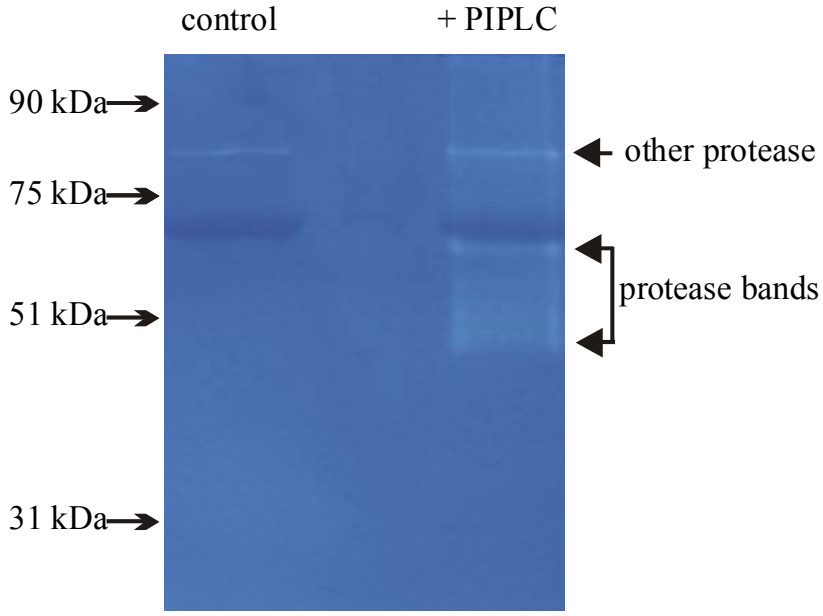

Figure 6: protease gel of PIPLC treated and control sciatic nerve. Protease bands are visualized as clear bands

The protease gel shows several protease activities in the gel. One band with a MW of about 80 kDa is similar in both control and PIPLC treated samples. But a smear of protease bands with a MW between 45 and 60 kDa appears in the PIPLC treated, but not in the buffer control. It is likely that the real MW of the protease is around 45 kDa, the smear resulting from proteolytic activity during the migration. This was the first evidence that indeed a GPI-anchored protease is present in the sciatic nerve. A major obstacle for purification of any protease is that autoproteolysis can occur resulting in low stability of the protein during the purification procedure. In my case, extensive use of protease inhibitors was precluded, because the assay, a protease gel, detected the proteolytic activity of the protein. I therefore decided to establish another assay to monitor this protein. The assay was based on the hypothesis that this protein interacts with BNC1 like CAP-1 interacts with ENaC. A rapid way to test for such an interaction is the Biacore system using surface plasmon resonance.

3.1.1 Binding studies using SPR

Before starting the binding experiments, recombinant BNC1a-nFLAG was purified from a permanent cell line expressing BNC1a-nFLAG using a affinity column with immobilized anti-FLAG antibody.

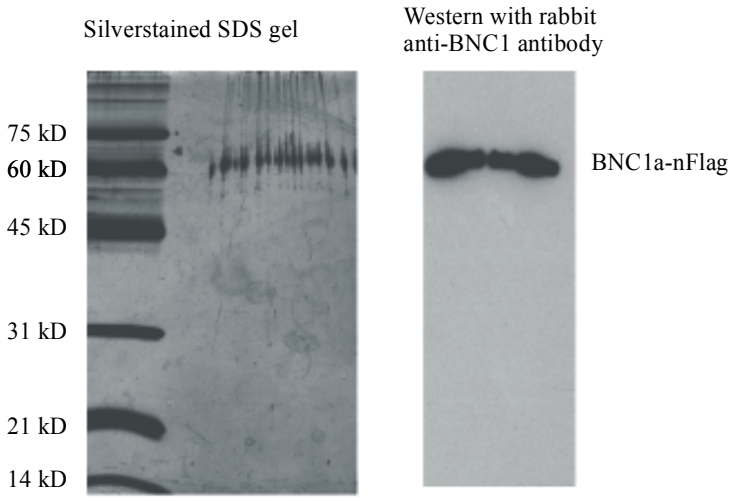

Figure 7: silverstained SDS-PAGE gel and western of purified BNC1-nFlag

Purified BNC1a-nFLAG was immobilized onto Biacore protein chips.

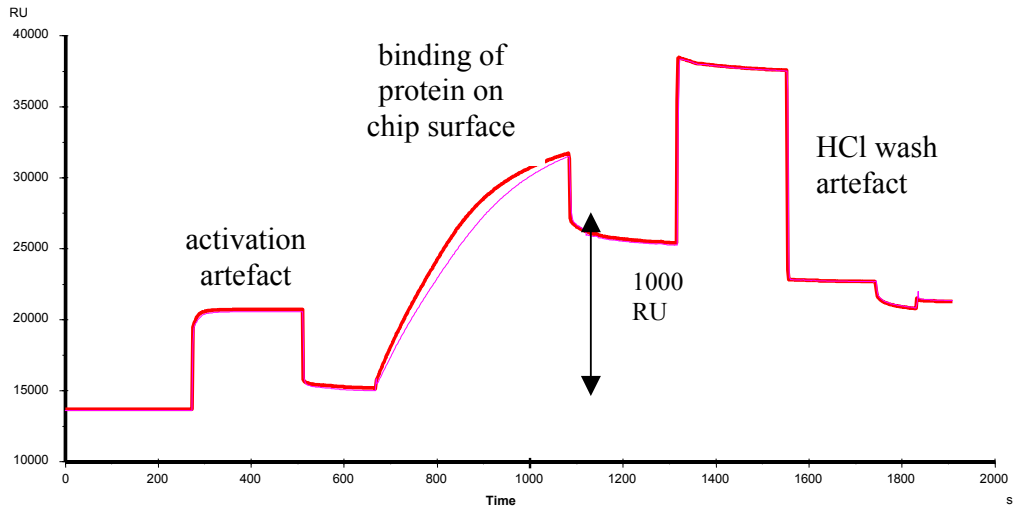

Figure 8: Sensorgram of BNC1 immobilisation onto a Biacore chip. The sensorgram shows the change of RU (response unit). The square shaped changes of RU before and after the binding phase results from changes of the chip surface properties during the surface activation and HCl wash procedure respectively.

The sensorgram shows the effective immobilisation of BNC1a protein onto the chip surface. The RU (response unit) difference of 1000 corresponds to about 1 ng/mm^2 of bound BNC1a protein. For binding experiments, test samples were applied onto the Biacore chip and binding activity was monitored.

First, sciatic nerve was treated with PIPLC or buffer control and the supernatants were tested.

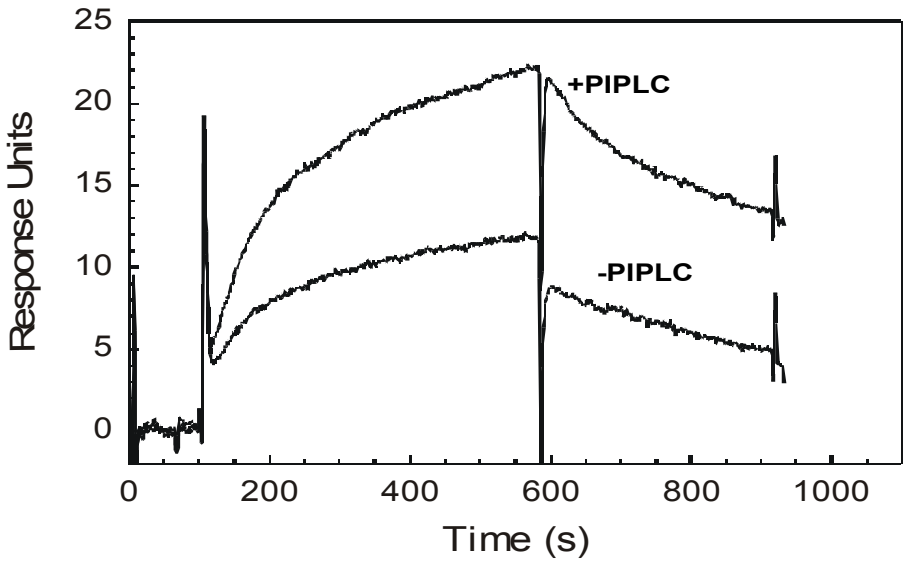

Figure 9: Increasing BNC1a binding activity after treatment of the sciatic nerve with PIPLC (this Biacore experiment was carried out by Anders Nykjaer at the Dept of Medical Biochemistry, University of Aarhus, Denmark.)

The sensorgram shows increased binding to BNC1a after PIPLC treamtment. It was still unclear whether this binding activity arose from a protease, but due to lack of alternative assays, I decided to use the Biacore binding assay as the standard assay for further purification steps. Another major problem was that for a successful purification the amount of starting material was too small. Since the skin is highly innervated by sensory neurons, I tested skin tissue of mouse for increased BNC1a binding activity after PIPLC treatment. For binding experiments, skin from rat foot was homogenized and treated with Triton X-114 to enrich for GPI anchored proteins (Bordier, 1981). An aliquot of the detergent phase was treated with PIPLC to release GPI-anchored proteins into the aqueous phase.

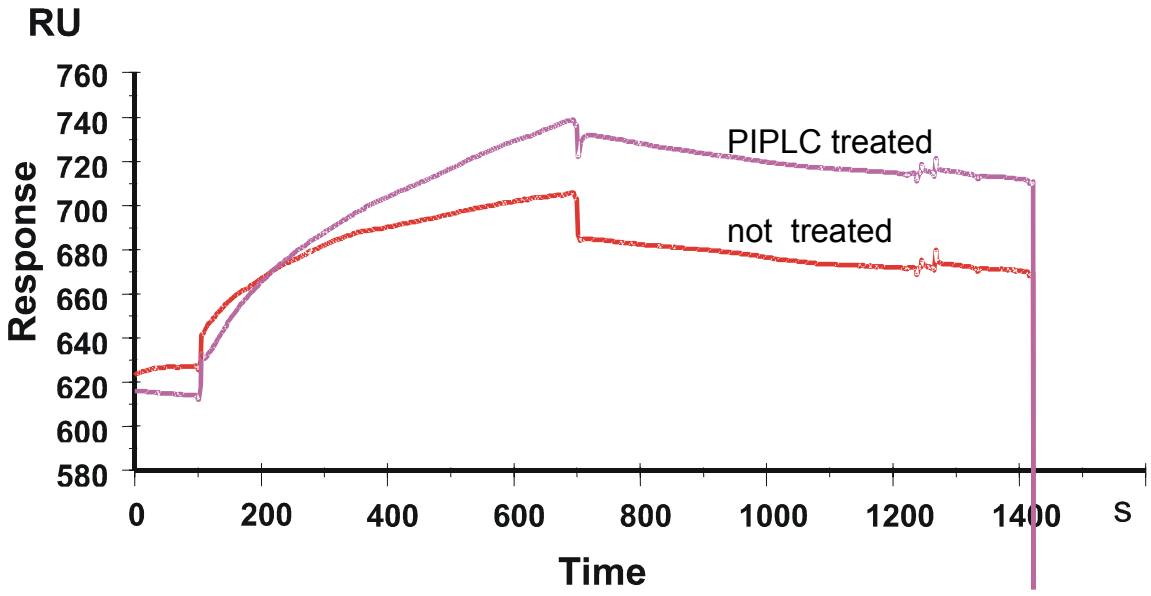

Figure 10: Increasing BNC1a binding activity after PIPLC treament of mouse skin

The sensorgram demonstrated an increased binding activity after PIPLC treatment in skin. For further purification, skin tissue was taken as starting material. In the first purification step the probe was applied onto a heparin column. Fifty millilitres of the aqueous phase following PIPLC treatment was applied onto the heparin column (HiTrap Heparin 5 ml, Amersham Pharmacia Biotech) using a fast protein liquid chromatography (FPLC) system (BioLogic, Biorad). Heparin-binding components were eluted using a salt gradient of 20 mM to 2M NaCl in 50 mM Tris and collected in fractions of 1 ml.

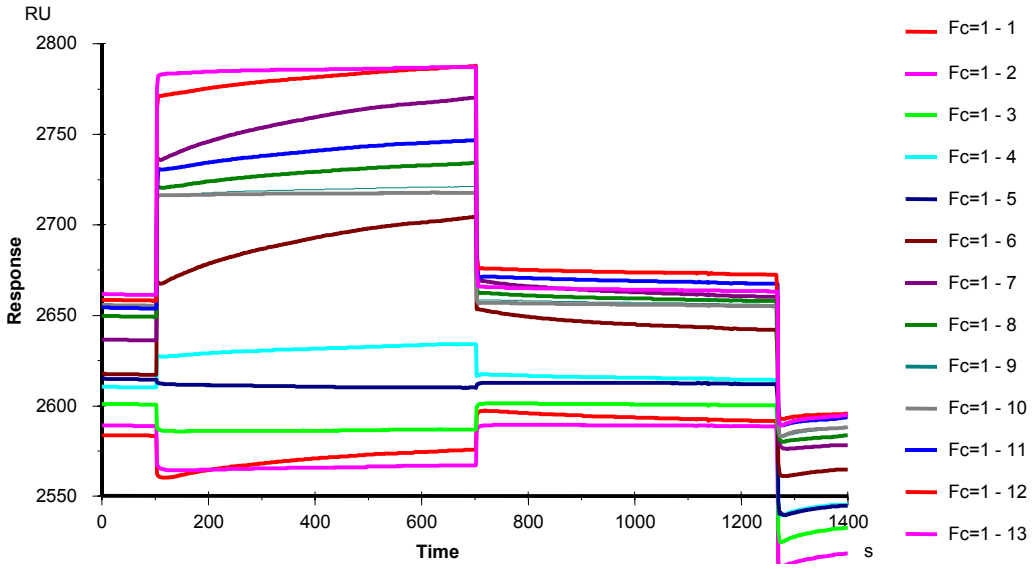

Figure 11: BNC1a binding activities of different fractions eluted from the heparin column

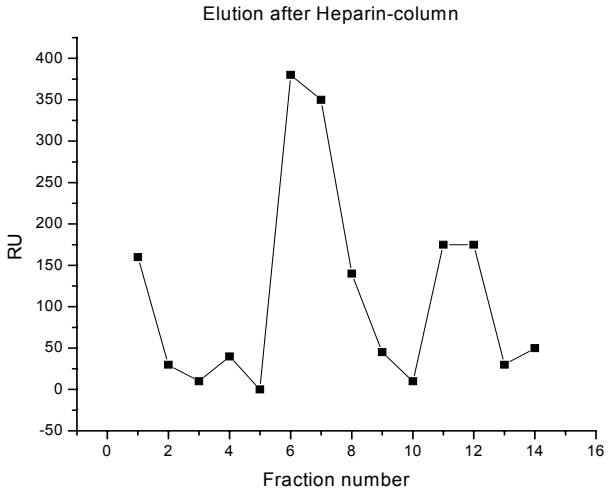

Figure 12: BNC1a binding activities plotted against eluted fractions

Two peaks with strong binding activity were located in fractions 6-8 and 11-12. Each fraction group was pooled and 3 ml of each was loaded onto a gelfiltration column (HiLoad 16/60 Superdex200, Pharmacia Biotech) for size fractionation. In total, more than 80 fractions were collected, and every 5th fraction was tested for BNC1 binding activity. Before injecting the samples onto the Biacore chip, the protein concentrations of all test fractions were determined and adjusted to equal levels in order to avoid differences due to variation in the protein concentration.

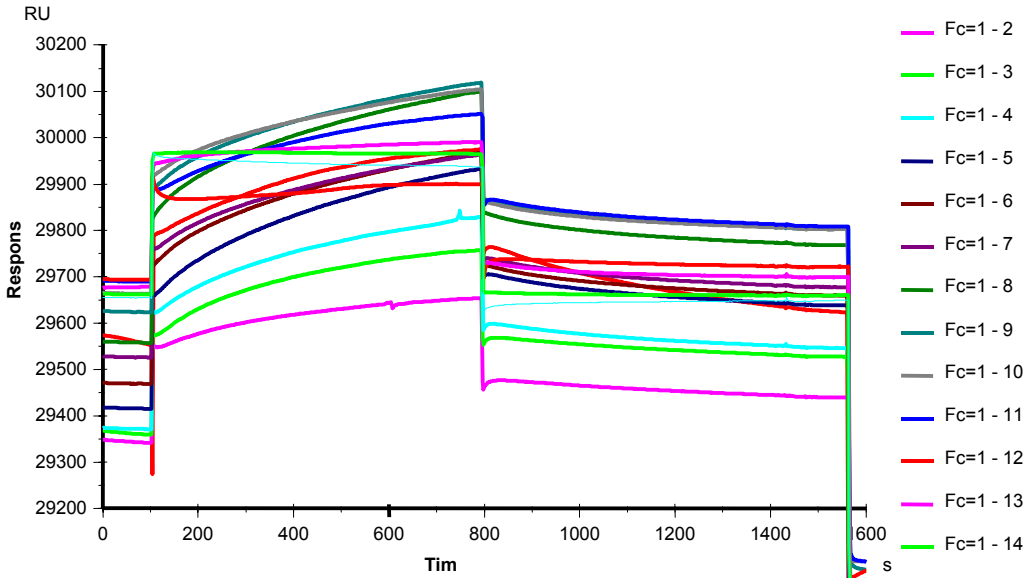

Figure 13: BNC1a binding activity of eluted fractions after gelfiltration

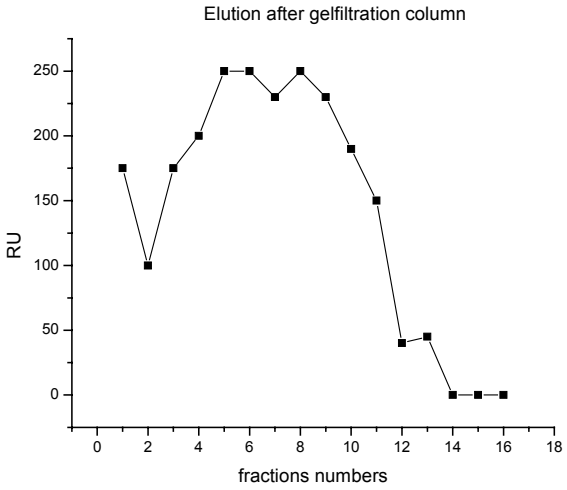

Figure 14: BNC1a binding activities plotted against eluted fractions

Most of the eluted fractions from the gelfiltration showed binding activity to the BNC1a protein. Thus, the gel gelfiltration methodology failed to separate the binding activity in a defined fraction, although the SDS PAGE analysis of fractions showed good size separation (data not shown). The fact that the binding activity was dispersed over the whole molecular weight range indicated that much of the binding signal might be unspecific. It was concluded that the Biacore assay was not suitable for further purification. The PIPLC released binding activity shown in figure 9 and 10 is probably too small to be detected against the background of unspecific binding activity. Control experiments were carried out to confirm the specificity of the binding using DTT (Dithiotreitol)-denatured BNC1a. DTT-treatment should denature the immobilized protein

resulting in reduced binding activity. Preinjection of DTT to the Biacore chip did not change the binding properties, indicating that most of the binding might be unspecific or alternatively, the native protein structure is not necessary for binding. In addition, samples from other organs like heart and lung also showed strong binding.

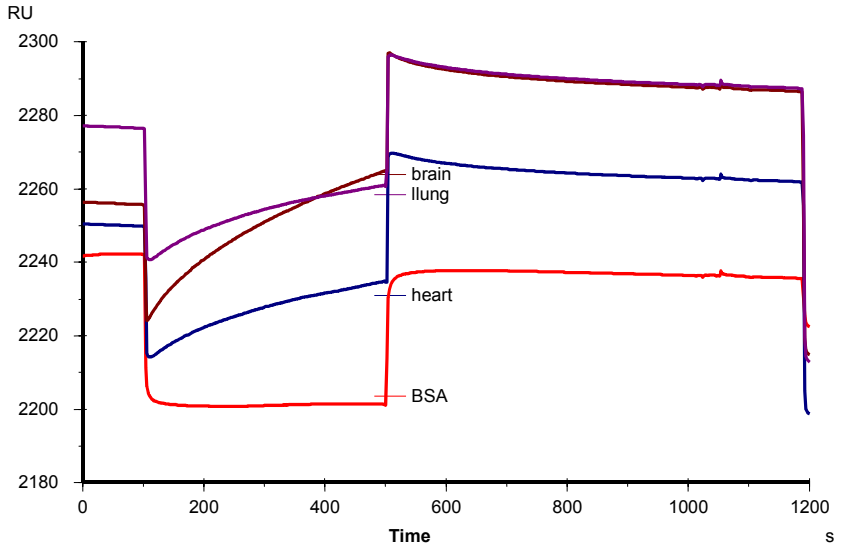

Figure 15: BNC1a binding activity of different tissues (after TX-114 treatment and PIPLC treatment)

Since BNC1 expression is restricted to the nervous system, any interacting factors from other tissues probably result from unspecific interactions. The binding signals seen with samples of two control tissues (heart, lung) therefore indicate unspecific binding activity in these tissues. The BSA control (containing 10 x protein concentration) showed that binding is not dependent on protein concentration. Nonspecific binding to BNC1a may be due to binding to hydrophobic regions on BNC1a, e.g. the transmembrane domains. I therefore generated a permanent cell line expressing a mutated BNC1a (BNC1a-ex or mdeg1-ex), that lacks both C- and N-termini containing the hydrophobic transmembrane domains. I planned to immobilize this mutated BNC1-ex protein onto Biacore chip and use it for binding assay, in order to decrease unspecific binding in the Biacore system. However, the recombinant protein proved difficult to purify. Meanwhile other column chromatographic methods were used for better fractionation (e.g. lectin columns, protease inhibitor columns, anion exchanger columns, data not shown), but results were inconclusive. Finally, mainly due to a lack of a convincing detection assay, I decided not to pursue this project further.

3.2 Search for BDNF-regulated mechanotransduction genes

Carroll and colleagues have previously shown that slowly-adapting mechanoreceptors in mice heterozygote for a BDNF null mutation are severely impaired in their mechanosensitivity (Carroll et al., 1998). Whereas the homozygote BDNF knockout mice die within 2-3 weeks after birth, the heterozygotes are normal and do not show any cell loss in the DRG besides the defect in low threshold mechanotransduction. We therefore hypothesized that BDNF regulates the expression of genes that are involved in mechanotransduction. Because only slowly adapting (SA) low threshold mechanotransduction are affected, we expected that BDNF is needed for the proper expression of genes, that are specifically expressed in SA neurons. SA neurons comprise about 20-40 % of large diameter DRG neurons. In order to find genes that are downregulated in DRG neurons of BDNF heterozygote mice, we combined expression analysis using Affymetrix gene chips (MG U74, 36 000 genes) with a suppression subtractive hybridization method.

3.2.1 Oligonucleotide array analysis

Total RNA from DRG of all spinal levels was prepared from 4-6 mice (on average 40 DRG per animal) per experiment and group. Biotin labeled cRNA for chip hybridization was prepared according to manufacturers protocol.

	BDNF WT			BDNF +/-		
	1.exp	2.exp	3.exp	1. exp	2. exp	3.exp
Number of animals per experiment	5	4	6	5	4	6
Yield of total RNA	128 µg	79 µg	100µg	85µg	86 µg	120µg
Amount of labelled RNA in Hyb.cocktail	30 µg/ 400 µl	25 µg/ 400 µl	25µg/ 400 µl	30 µg/ 400 µl	25 µg / 400 µl	25µg/ 400 µl
Test chips	ok	not used	not used	ok	not used	not used

Table 1: The table indicates the number of animals, total RNA yield and amount of labeled cRNA that was used for the experiments. Experiments were performed in triplicate.

Labelled cRNA was hybridized to commercially available Affymetrix oligonucleotide array Mouse Genome U74 set. After the first two experiments were completed, Affymetrix announced a manufacturing defect. The mouse genome U74 chip set (MG U74) that was used for our experiments consists of three chips (chip A, B. C), containing in total 36000 transcripts. Around 33% of the sequences on the chips (20% of chip A, 24% of chip B and 55 % of chip C) were in antisense orientation due to incorrect sequence downloads from the public database, that were

used as basis for oligonucleotide design. Data belonging to false oligonucleotides were discarded and all experiments were repeated once more using the corrected MGU74 version2 arrays. Consequently, the first two experiments covered only about 24000 putative genes instead of 36000 genes.

The Affymetrix array technology provides built-in quality control features which control cRNA sample integrity by measuring the expression level of the 5', middle and 3' region of three house keeping genes (glycerolaldehyde-3-phosphate dehydrogenase, β-actin and hexokinase). In all experiments, signal ratios of 3´and 5´region of all housekeeping genes were within an acceptable range (3`/5`ratio beween 1 and 3).

Analysis of the hybridization was carried out using the Data Mining Tool software from Affymetrix. In all experiments, about 35% of the genes on the chip were called as present. This is the range that is normally expected from a complex tissue. Since the genes I was looking for might be called absent by the Affymetrix software due to their low abundancy, I decided not to consider the absolute call (present, absent or marginal). Therefore only the fold change was used for selecting regulated genes. Taking this criterion, 142 genes were downregulated in all three experiments (fold change < -1,4). BDNF, that should be theoretically downregulated 2 fold, was downregulated only 1,3 fold in the heterozygote in comparison to the WT. This indicates that the fold changes determined by Affymetrix experiments are perhaps underestimates of the real values.

3.2.2 Suppression subtractive hybridization

I was looking for genes that are specifically expressed in SA mechanoreceptors. Around 30 % of all DRG neurons are large diameter neurons, from which SA mechanoreceptors make up about 20-40 %. Consequently, SA mechanoreceptors comprise only about 10% of all DRG neurons. It is therefore quite likely that the Affymetrix cDNA array might not detect rare transcripts specifically expressed by SA mechanoreceptors. We therefore decided to strengthen our screen by using the suppressive subtractive hybridisation technique to generate a subtractive cDNA library of transcripts downregulated in the DRG of BDNF heterozygote mice. BDNF heterozygote mice lose their low threshold mechanosensitivity without any other accompanying sensory defects, therefore I assumed that the set of differentially expressed genes between WT and heterozygote mice would be small. In general, the false positive background of subtraction experiments, that means the number of genes which are present in the subtracted library without being differentially expressed, is higher the more similar the two RNA samples are. Therefore, I expected a high percentage of false positive clones to be present in the subtracted library. The

subtraction technique provides an internal unsubtracted control, representing the sum of both RNA pools. To start the subtraction procedure, DRG from all spinal levels from 2 mice heterozygote for BDNF and 2 WT mice were taken (on average 40 DRGs per animal) and RNA extracted using the Trizol method. The Smart PCR cDNA amplification kit and the PCR Select kit by Clontech were used to perform cDNA amplification and the subtraction procedure. The subtraction efficiency was controlled by comparing the abundancy of GAPDH in subtracted and unsubtracted control samples. GAPDH abundance in subtracted sample was about 20 times lower than in unsubtracted control, confirming that common genes like GAPDH are reduced in the subtracted sample. The subtracted library and the unsubtracted control library were converted to biotin-labeled cRNA and hybridised onto Affymetrix chips. Genes that were present in the subtracted library and absent in the unsubtracted control were defined as real positives. Using this analysis, 283 genes were identified as specifically present in the subtracted library.

3.2.3 Combined analysis

From 142 genes, that were downregulated in the Affymetrix study, only 2 genes were also present in the group of 284 genes of the subtracted library. This is a very poor overlap of the Affymetrix and the subtraction experiment. One might expect one overlapping gene even if the 283 genes in the subtracted library and the 142 downregulated genes in the Affymetrix experiment were picked randomly. However, it was interesting that both genes that fitted our most stringent criteria were actin binding genes.

1.) AW045218: filamin like protein (Affymetrix ID: 97300_at)
2.) AW121640: WAVE3 (wasp-like protein) (Affymetrix ID:111261_at)

Because it was obvious that the reproducibility of the experiment was too poor to use very stringent selection criteria, I decided to decrease the selection stringency and to consider genes that were downregulated in at least two of three Affymetrix experiments and were present in the subtracted library. Cellular expression of some of these genes were analyzed using in-situ hybridization.

3.2.4 In situ hybridization

Our aim was to find genes that are specifically expressed in slowly adapting (SA) mechanoreceptors. Slowly adapting mechanoreceptors are a subgroup of large diameter neurons, therefore I determined the cellular expression of some of the candidate genes in order to look for genes that are expressed in large diameter neurons and are downregulated in BDNF heterozygotes.

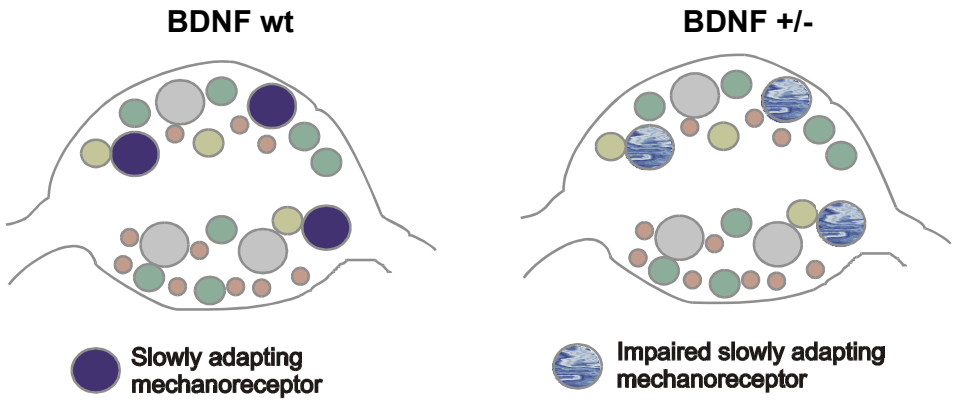

Figure 16: Scheme of expected in situ hybridization expression pattern. SA mechanoreceptor specific genes should be expressed in medium sized DRG neurons and downregulated in BDNF +/- mice.

So far, I have performed in situ hybridization of 5 candicate genes (AW 124164, AI 156978, AI 843650, AI 852174, U65592 (k-channel, β-subunit)). Most genes were expressed in all neurons, only U65592 (β-subunit of a potassium channel) was specifically expressed in medium to large diameter neurons. But none of these genes showed reduced number of stained cells in BDNF heterozygote mice.

So far, using this screen I was not succesful in identifying genes specific for slowly adapting mechanoreceptors. However, there are still many genes including the two actin binding proteins, which still need to be analyzed using in-situ hybridization, therefore it is too early to judge the success of the experiment. The expression data is still interesting in context to the second series of expression profiling experiment, in which I searched for NT-4 regulated genes. Both neurotrophins share the same cellular receptor, and it is therefore interesting to see whether the group of BDNF regulated genes overlap with NT-4 regulated genes.

3.3 Search for D-hair specific genes

Of all mechanoreceptive neurons in the DRG, the so called D-hair mechanoreceptors are of particular interest, as they are the most sensitive mechanosensors (Burgess et al., 1968; Brown et al., 1967 a, b; Koltzenburg et al., 1997) therefore serve as a prototype for mechanoreceptive neurons. Recent studies showed that this receptor type, which comprises around 5-7 % of DRG neurons, is almost completely lost in neurotrophin-4 (NT-4) null mutant mice (Stucky et al. 1998). By identifying genes that are downregulated in the mutant mice we hoped to find genes that are specific to or highly enriched in D-hair mechanoreceptors.

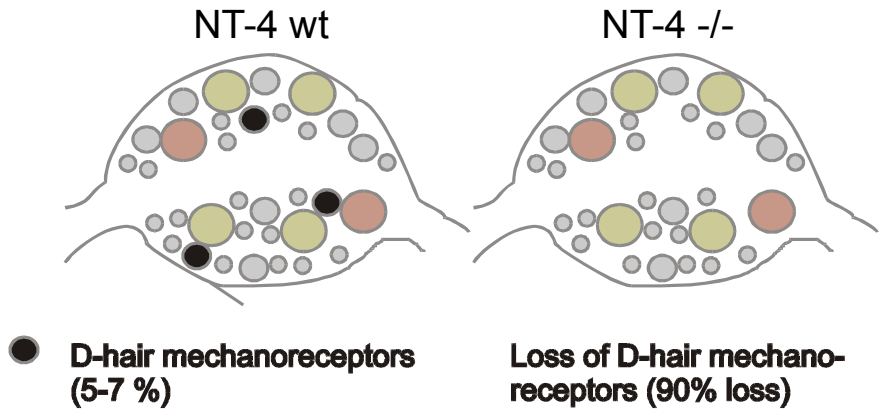

Figure 17: scheme of expected expression pattern of D-hair mechanoreceptor specific genes in DRG. D-hair receptors have intermediate size cell diameter and comprise around 6% of all DRG neurons. NT-4 knockout mice almost completely lack D-hair receptors

3.3.1 Apoptosis in adult NT4 null mutants

The study of Stucky and colleagues did not show loss of D-hair mechanoreceptors in NT-4 ko mice directly. There are no markers for D-hairs available and the number of D-hairs in the DRG is too small to show a specific loss of this cell type by counting all neurons in the DRG. Instead, Stucky demonstrated the loss of D-hair receptors using eletrophysiological recordings with the skin-nerve preparation. The absence of physiologically identifiable D-hair receptors was confirmed by histological studies of the saphenous nerve where a subset of thinly myelinated axons was missing in the mutant mice. One potential problem with this analysis is that the receptor ending and the axons are lost but the cell body might still be intact. Since loss of neurons was a necessary criterion for a success of my expression studies, I first wanted to prove that cells are really lost in NT-4 knockout mice through apoptosis. Electrophysiological studies

showed that D-hair receptors are present in young NT-4 knockout mice and start to disappear between the 7th and 10th postnatal week, probably due to apoptosis as a consequence of lack of NT-4 supply in this critical period. In order to show apoptosis I performed TUNEL staining on DRG paraffin sections from 8 week old NT-4 null mutant and WT mice. Three animals were examined per group, about 40 DRGs per animal. In total about 700 DRG sections per group were examined for TUNEL positive cells.

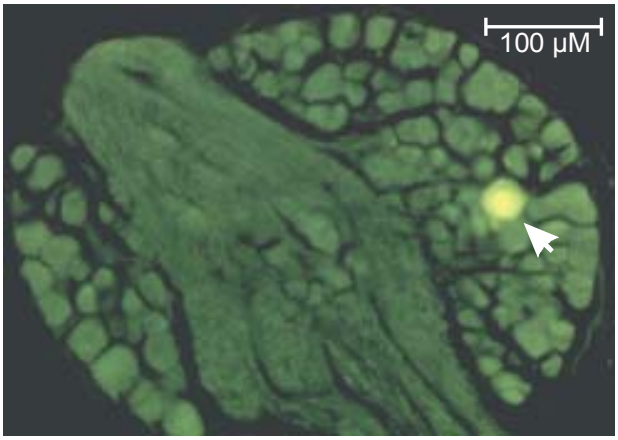

Figure 18: TUNEL staining in DRG sections of 8 weeks old NT-4 knockout mice. The arrow indicates a representative TUNEL positive neuron.

	WT (8 WEEKS PN)	NT-4 -/- (8 WEEKS PN)
total number of counted neurons	750	770
total number of TUNEL positive neurons	0	5

Table 2: Quantification of TUNEL positive neurons in wt and NT-4-/- mouse DRG. As expected the level of apotosis was low because D-hair receptors comprise only 6% of DRG neurons and are lost over a long time course.

TUNEL positive cells were exclusively found in NT-4 knockout mice and not in WT indicating that neurons are indeed lost in NT-4 knockout mice through apoptosis.

In order to find genes that are downregulated in DRG of NT-4 null mutants in comparison to the WT, we combined expression analysis using Affymetrix gene chips (MG74, 36 000 genes) with a suppression subtractive hybridization method.

3.3.2 Oligonucleotide array analysis

For Affymetrix expression studies, I dissected out DRGs of all spinal levels from WT and NT-4 knockout mice (about 40 DRGs per animal). Experiments were performed in triplicates, each experiment independently with new mice. Fluorescently labeled cRNA was prepared according to the Affymetrix Manual.

	NT4 WT			NT4 KO 5W			NT4 KO 12W		
	1.exp	2.exp	3.exp	1. exp	2. exp	3.exp	1.exp	2.exp	3.exp
Number of animals per experiment	10	10	12	10	10	12	10	10	12
Yield of total RNA	120 µg	120µg	130µg	125µg	120µg	140µg	92 µg	100µg	145 µg
Amount of labelled RNA in Hyb.cocktail	30 µg/ 400 µl	30 µg/ 400 µl	21µg	30 µg/ 400 µl	30 µg/ 400 µl	21µg	30 µg/ 400 µl	30 µg/ 400 µl	21µg
Test chips	ok	ok	no	ok	ok	not used	ok	ok	not used

Table 3: The table indicates the number of animals per experiment, yield of total RNA and amount of labelled cRNA that was used for the hybridisation on Affymetrix chips

Labelled RNA was hybridized to the commercially available Affymetrix oligonucleotide array Mouse Genome U74 set. The signal ratios of 3´ and 5´region of all housekeeping genes (glycerolaldehyde-3-phosphate dehydrogenase, β-actin and hexokinase), that indicates the RNA quality, were within an acceptable range (3`/5`ratio beween 1 and 3).

As in the BDNF experiment, I decided not to consider the absolute call (present, absent or marginal) and to take only the fold change of the comparisons. Due to the inevitable variability during the dissection procedure I expected that random variation between the experiments might be high. This was the case. None of the genes were decreased in all 6 experiments (3 experiments comparing the expression of WT against 12 week old NT-4 ko mice and 3 experiments comparing the expression of 5 week old NT-4 ko mice against 12 week old NT-4 ko mice). Therefore we decreased the stringency for candidate genes and selected genes that showed downregulation (fold change > -1,4) in 4 of 6 experiments. 195 genes met this criterion.

3.3.3 Suppression subtractive hybridization

Like the BDNF experiment this experiment faces the potential problem that interesting genes might be rarely expressed transcripts (D-hair receptors comprise only around 5% of DRG neurons). We therefore decided to strengthen our screen by using the suppression subtractive hybridisation technique to generate a subtractive cDNA library of transcripts downregulated in the DRG of NT-4 knockout mice. In principle, two subtractions could have been performed: 1.) NT-4 WT and old NT-4 knockout and 2.) young NT-4 knockout and old NT-4 knockout. I chose to subtract the cDNA of WT from the old NT-4 knockout mouse. An aliquot of the total RNA from the first NT-4 Affymetrix experiment was taken as starting material. The amplification and subtraction procedure was performed according to the manufacturers protocol (Smart kit and PCR-Select kit from Clontech). Both the subtracted and the unsubtracted control library were converted to biotin-labeled cRNA and hybridized onto Affymetrix MGU74 chips. I looked for genes that showed high hybridisation signals in the subtracted but not in the unsubtracted control. The results were sorted for high average difference in subtracted and low average difference in the unsubtracted control and the first 1000 in this list were defined as most likely to be differentially regulated.

3.3.4 Combined analysis

From 195 genes that were downregulated in at least 4 of 6 Affymetrix experiments, 28 were also present in the subtracted library. As in the BDNF experiment, the overlap of the two approaches might appear low. But the subtraction procedure can detect differential expression of low abundant genes, whereas the regular gene array experiment may fail to detect such genes. In addition, the Affymetrix study is restricted by the number of chosen oligonucleotides. Therefore the low overlap of the results of these two experiments is not only due to experimental variation, but is also based on the principally different output focus of these two approaches.

For further analysis, we focussed on the 28 genes that appeared to be differentially downregulated in both experiments. In addition we chose a few genes that were strongly represented in the subtraction library but not detected in the regular Affymetrix study and a few genes, that did not meet these stringent criteria but appeared interesting for other reasons e.g. an already reported regulation by neurotrophins.

Except for 4 genes that I could not amplify from DRG cDNA, fragments of all genes of interest were succesfully PCR amplified from a mouse DRG cDNA and cloned into pGEM-T plasmids.

					FOLD CHANGE COMPARED TO NT4 -/- 12W	IN-SITU HYBRIDISA

					1. Exp		2. Exp		3. Exp		TION: **e**: expressed **ne**: not expr. **c**: changed in ko vs wt **nc**: no chang
	Affymetrix ID	Accession number	Blast result	Abs call in 3 WT exp	wt	-/-5w	wt	-/-5w	wt	-/-5w	
chi pA	96239_at	AA 815503	Similar to VRK1	P/P/P	-1,5	-1,5	-1,5	-1,4	-1,2	-1,3	e, nc
	96302_at	AA711516	Similar to splicing factor	P/P/P	-1,6	-1,9	-1,9	-1,4	-2,3	-1,7	e, nc
	96346_at	AI 854020	Novel, PTR repeats	P/P/P	-1,4	1,1	-1,7	-1,4	-1,6	-1,8	e, nc
	160953_at	**AF051947**	**CaV3.2**	**A/A/A**	**-1,5**	**-1,5**	**-2,2**	**-1,4**	**1,2**	**-1,4**	**e, c**
	102561_at	U59282	F1F0 ATP-synthetase	P/P/P	-1,5	1,3	-1,1	-1,7	-1,4	-1,5	e, nc
Chi p B	103787_at	Y00305	Kv1.1	P/P/P	-1,1	-1,2	-2,7	-6,3	-1,2	-2,5	e, c
	105043_at	ai 615578	Mouse RAD52	A/P/A	1,2	2	-1,6	-2,1	-1,7	-2,4	e, nc
	105063_at	aa727468	No match	P/P/P	-1,1	-1,5	-2,4	-2,8	-1,5	1,1	e, nc
	105572_at	aa 822744	Mitogen induced orphan receptor	A/A/A	-1,7	-2,6	-1,6	-2,3	1,9	1,4	weak
	107372_at	aa763786	Similar to teashirt2	A/P/A	-1,9	-3,0	1,4	-1,5	-2,1	1,2	e, nc
	109447_at	aw 209204	No match	P/A/A	-1,7	-1,7	-1,6	-1,6	-1,2	1,2	e, nc
	110526_at	aw 146415	No match	A/A/A	-1,4	-1,5	-1,5	-3,4	-1,4	1,5	not cloned
	111492_at	aw 121484	CACNA 2D1	A/A/A	-2,3	-1,9	-1,2	-1,6	1,9	-2,8	ne
	111651_at	aw 208446	KIAA0644	A/A/A	-1,5	-1,8	-1,2	-2,2	-1,9	1,7	e, nc
	112985_at	ai 530426	Secreted phospholipase2	A/M/A	-1,3	-1,3	-2,2	-1,7	-1,8	-1,6	e, nc
	113309_at	ai 882298	Similar to KIAA0189	P/P/A	-1,7	-3,0	-2,3	1,4	-1,8	1,1	e, nc
	114733_at	ai 608482	No match	P/P/A	-1,4	-1,7	-2,1	-2,7	-3,9 D	3,8 I	not cloned
	114815_at	ai 55547	No match	P/A/P	-1,1	-1,1	-1,6	-1,5	-1,9	-1,7	not cloned
	114848_at	ai 852283	Similar to a serine protease	A/A/A	-2,0	-1,4	1,2	-2,5	-2,8	-2,9	e, nc
	115332_at	ai 551483	No match	A/A/P	-1,7	-1,5	-1,9	-2,3	-1,3	1,1	e, nc
	115829_at	aa 939463	Similar to FLJ00248	A/A/A	-1,0	1,3	-2,2	-1,5	-1,5	-1,9	e, nc
Chi p C	135180_at	ai 021510	Similar to zinc finger protein 151	A/A/A	-1,6	-1,4	-2,5	-1,6	-3,1	-1,8	e, nc
	139755_at	ai 448778	TEF-5 transcriptio factor	A/A/A	1,7	-1,5	-1,6	-1,6	1,8	-1,8	e, nc
	141026_at	aa 544572	No match	P/P/P	-1,6	-1,5	-1,9	-1,7	-1,7	-1,0	not cloned
	131279_at	Ai 480618	Similar to TFII-I	P/P/P	-1,4	-1,5	-1,0	-1,1	-1,6	-2,2 D	e,nc

	134153_at	aa 210488	No match	A/P/A	1,0	-1,5	2,1	-1,7	-1,6	-1,6	e, nc
	135118_at	ai 463032	No match	A/A/A	-2,1	-2,4	-2,1	-2,7	-1,5	-3,3	e, nc
	138452_at	**AI836811**	**TrkB**	**P/P/P**	**-1,4**	**-1,1**	**-1,7**	**-1,1**	**-3,2**	**-3,3**	**E,c**

Table 4: The table lists the 28 genes that were downregulated at least 1,4 fold in 4 of 6 Affymetrix experiments (3x WT vs old NT-4 -/- and 3x young vs old NT-4 -/-) and present in the subtracted library. No match means there was no match to sequences in the public database (GenBank), unknown indicates a match to a gene of unknown function. In situ column: exp= expressed in DRG neurons, nc: no change of expression pattern in old NT-4 ko mouse. c clear change of expression pattern (reduced number of stained neurons) in old NT-4 -/- mouse. not cloned: cDNA could not be be amplified from mouse DRG mRNA with RT-PCR.

Some other genes were present in the subtracted library but were not downregulated in the Affymetrix study. These genes are likely to be downregulated but failed to be detected in the Affymetrix study due to low abundance. Two of them, called Nip21 (AF035207) and Desmin (L22550) were cloned from mouse DRG cDNA.

Affymetrix ID	Accession number	Blast result	Abs call in 3 WT experim.	Fold change in						In-situ hybridisation
				1. Exp		2. Exp		3. Exp		
				wt	5w	wt	5w	wt	5w	
		VAMP								**e, nc**
97520_at	X83569	neuronatin	P/P/P	-1,3	-2,1	-2	-2,6	-1,8	1,5	**e, nc**
140639_at	AW060690	HAC1 (hyperpol. activ. chan)	P/P/P	-1,4	-1,4	-1,4	1	1,1	-1,2	**e, nc**
96583s_at	AF053473	Kinesin	P/P/P	-1,2	-1,9	-2,7	-4,4	-1,4	-2	**e, nc**
102988_at	U92477	AblSH3 binding protein	A/P/P	-1,7	-1,6	-1,8	-1,4	-1,4	-1,1	**e, nc**
93507_at	X62622	Tissue inhi. of metallo-proteinase	P/P/P	-1,2	-1,6	-2,4	-4,5	-1,6	2,2	**e, nc**
	AB018194	BIT	P/P/P	-2	-2	-2,1	-1,7	1	-1,2	**e, nc**
93727_at	AB003502	Guanine nucleot. regul. protein	P/P/P	-2,6	-2,1	-1,5	-1,9	-1,1	1,1	**e, nc**

Table 5: The table lists a subset of interesting genes that did not match all stringent criteria but appeared interesting. e: expressed; ne: not expressed; c: changed in ko vs wt; nc: not changed.

All above mentioned genes, except those that could not be cloned were examined for expression in mouse DRG using DIG-labeled non-radioactive in situ hybridization.

3.3.5 In situ hybridization

Expression analysis using gene arrays and DNA subtraction resulted in the identification of genes that are downregulated in the old NT-4 null mutants in comparison to the young null mutants and the WT mice. Genes that are downregulated in the old NT-4 null mutants compared to the young null mutants might reflect expression changes due to maturation. The genes that are downregulated in the old mutant compared to the WT mice could also be transcriptional downstream targets of NT-4 regulation. Genes that are downregulated in both groups are good candidates for specific expression in D-hair receptors since the loss of D-hair receptors is the common property in both comparisions. To finally examine the cellular expression of these genes we performed in situ hybridisation using non-radioactive DIG-labelled cRNA probes. The Affymetrix study and the subtraction experiment resulted in 28 genes that were potentially interesting. In addition around 20 other genes that were strongly represented in the subtracted library or highly significantly downregulated in the Affymetrix experiment were examined. Specific DIG–labeled probes were generated from cloned gene fragments and hybridized on DRG cryostat sections. The conditions for the in situ hybridisation were optimized for each gene individually, mainly by varying the probe concentration and hybridisation temperature. Optimized probe concentration ranged between 50-200 ng/ml and the hybridisation temperatures between 52°C-58°C. The expression patterns of the genes are indicated in the table above. Most genes showed neuronal expression in DRG, some of them displaying an interesting pattern of expression.

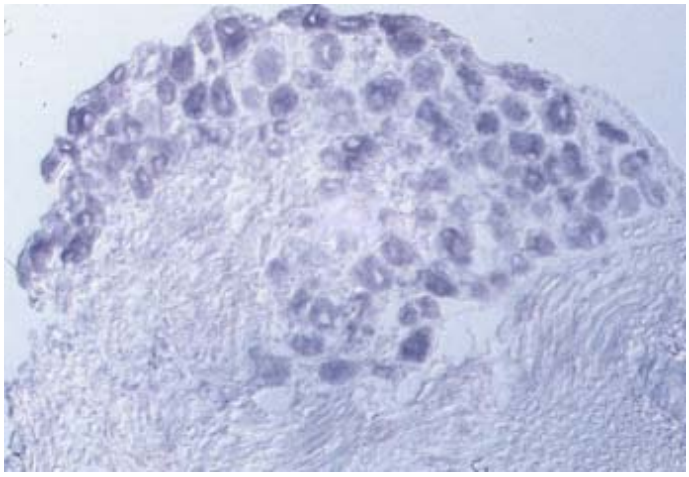

Figure 19: In-situ hybridisation of the gene with the Genbank accession number aa727468. Representative for all genes in the list, that were expressed in all neurons, but not downregulated in the NT-4 null mutant mice.

A few of the genes showed a very specific expression pattern:

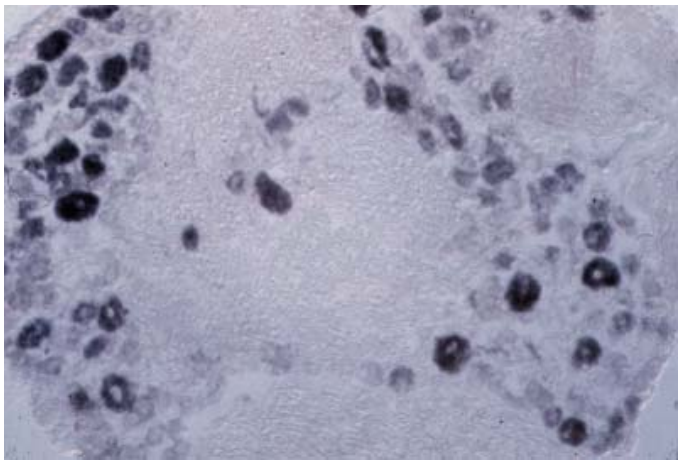

Figure 20: In-situ hybridisation of Kv1.1. Expression in medium to large diameter neurons

Kv1.1 is a potassium channel, that seems to be specifically expressed in large and medium sized neurons. When compared to the NT-4 null mutant mice, there was no obvious difference detectable (in situs not shown), but a loss of a subset of medium sized neurons might be too minor to be noticeable without quantification.
Another gene with an interesting expression pattern was neuronatin.

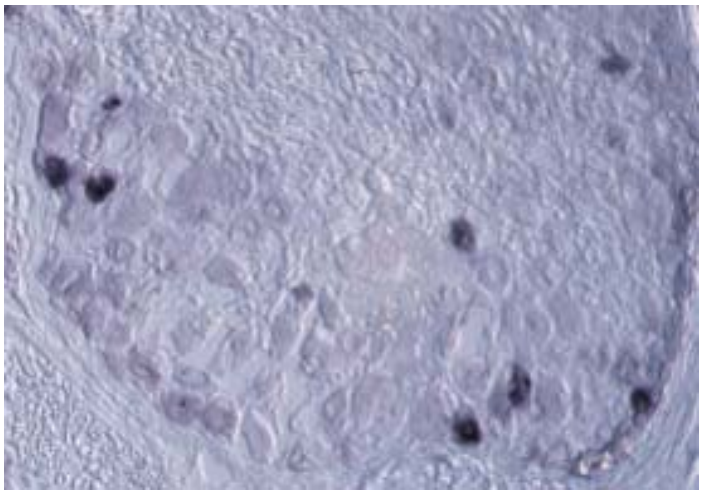

Figure 21: in-situ hybridisation of neuronatin. Expression in medium sized neurons, but no downregulation in old NT-4 null mutant mice.

Neuronatin is expressed specifically in medium sized neurons, but not downregulated in old NT-4 mutant mice. We can therefore conclude that neuronatin is not a D-hair specific gene, although it is expressed in medium sized neurons. It is known that neuronatin is highly expressed after birth and gets downregulated with maturation (Joseph et al., 1994). Since our screen also included an age dependent comparison, this might be the reason why neuronatin came up in our screen. It should also be noted that neuronatin was not present in the subtracted library, which makes sense, because the library was made by subtracting the old NT-4 null mutant from age matched WT mice. Medium sized neurons in the DRG are comprised of D-hairs or AM high threshold mechanoreceptors. We therefore can hypothesize that neuronatin is expressed in AM mechanoreceptors. But this remains to be proven.

Finally, the screen succeeded in the identification of two genes that exactly matched our criteria for D-hair receptor specificity. The first one was trkB, the cellular receptor of the neurotrophins BDNF and NT-4. This finding was not surprising since D-hair mechanoreceptors express trkB and a loss of D-hair receptors should therefore lead to a loss of trkB positive neurons.

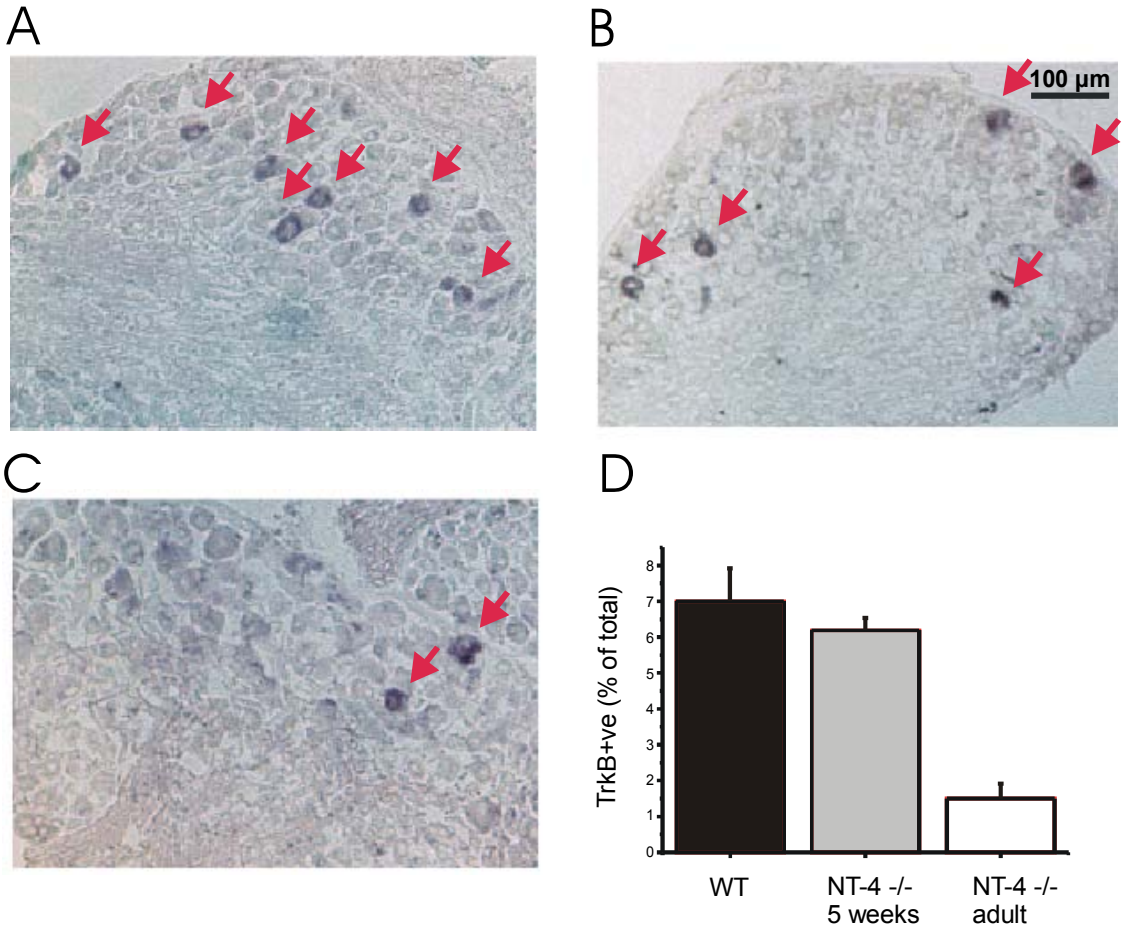

Figure 22: A: In-situ hybridisation of trkB in NT-4 wt, B: NT-4 -/- 4w, C: NT-4 -/- 12w; arrows indicate trkB positive DRG neurons; D: quantification of the percentage of trkB

positive cells over many different sections from two independent experiments. Note a significant reduction of around 78 % in positive neurons in adult NT-4 -/- mice compared to controls.

But the more interesting finding was that the T-type calcium channel CaV3.2 (Cribbs et al., 1998) was expressed in medium sized neurons and downregulated in old NT4 ko mice.

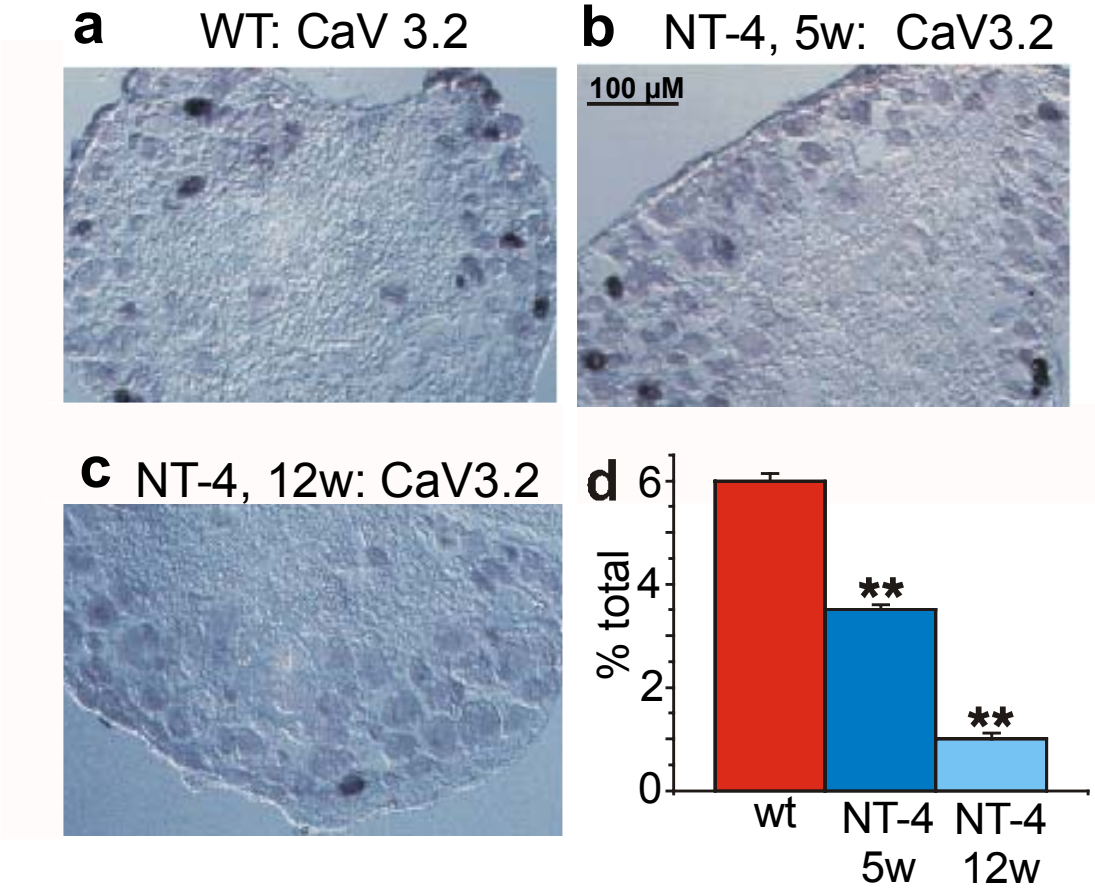

Figure 23: a: In-situ hybridistion of CaV3.2 in wt, b: NT-4 -/- 4w, C: NT-4 -/- 12w; d: quantification of CaV3.2 positive cells (indicates significant difference p<0.001 unpaired t-test)**

One can conclude that CaV3.2 is the first identified gene that is specifically expressed or at least highly expressed in D-hair mechanoreceptors.

3.3.6 Quantitative PCR

I performed real time PCR with some selected interesting genes to confirm the expression data. Specific primers and probes were designed for TrkB, Kv1.1, CaV3.2 and the other two T-type calcium channels, CaV3.1 and CaV3.3. Complementary DNA (cDNA) from wt, 4 week old NT-

4 null mutants and 12 week old NT-4 null mutants were taken as template. The amplification rate of all genes were normalized to GAPDH. All experiments were carried out in triplicate.

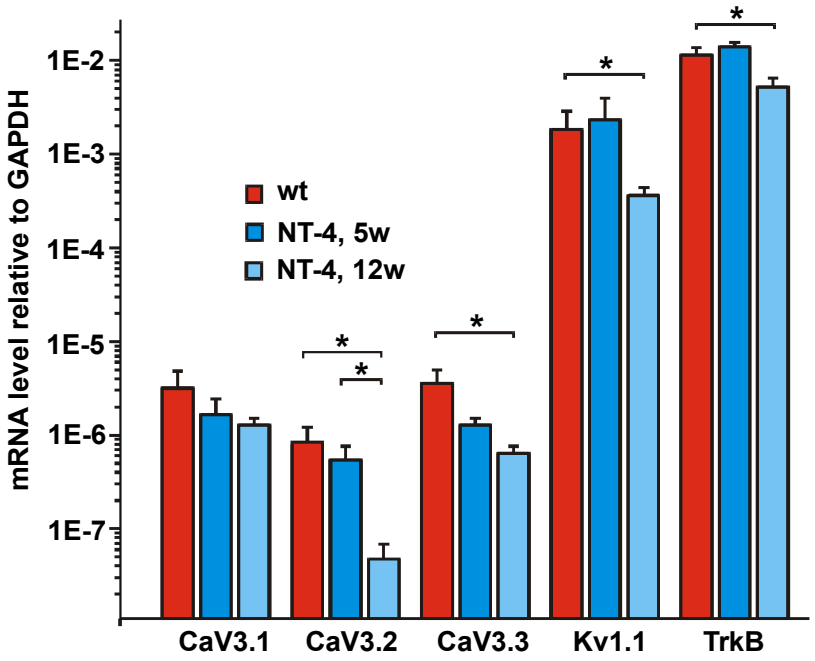

Figure 24: Real time PCR showing the relative abundance of CaV3.1, CaV3.2, CaV3.3, Kv1.1 and trkB normalized to GAPDH (* indicates a significant difference p<0.001 Mann Whitney U-test)

These results confirm the Affymetrix expression studies, but also provide new insights. In real time PCR experiments, trkB is downregulated about 3 fold in the old NT-4 mutants compared to the wt. This fold difference value lies between the result of the expression data, whereas an average difference of 2 fold was determined, and the in situ hybrisisation experiment that resulted in 7 % trkB positive cells in the wt and 1,5% in old NT-4 mutant mice (>4 fold difference). Also the real time PCR for Kv1.1 resulting in a four fold difference was in agreement with the Affymetrix data (mean fold change 2,5 fold), with a comparable age dependent downregulation of Kv1.1 transcript in NT-4 mutant mice. Kv1.1 is expressed mainly in large diameter neurons, but also in a few medium sized neurons. Although no obvious differences were detected in the in situ hybridisations, it is expected that a more detailed cell count analysis considering the cell size dependent distribution will show a difference. Kv1.1 may turn out to be interesting, since it is very specifically expressed in medium to large diameter

neurons and not in small neurons and therefore might help to figure out the differences between neurons mediating noxious and innocuous mechanotransduction. The real time PCR results of the three T-type calcium channels confirmed the in situ hybridization data and also provided some unexpected results. The profile of CaV3.2 transcript levels agree with the in-situ hybridization data, showing no difference between wt and young NT-4 mutant mice, but a more than 13 fold reduction in old NT-4 mutants. The transcript level of CaV3.1 is not changed, but surprisingly, the T-type channel subtype CaV3.3 is downregulated in NT-4 mutant mice, but in the absence of the striking age dependent difference seen in CaV3.2 expression. Based on this result I suggest that CaV3.3 is also expressed in D-hair receptors, but probably not exclusively like CaV3.2, since the profile of transcript levels for wt, young and old NT-4 null mutants does not match the criteria for D-hair receptors as well as for CaV3.2 or trkB.

3.3.7 Functional studies using skin-nerve preparation

Expression studies using in situ hybridisation revealed that the T-type calcium channel CaV3.2 was specifically expressed in medium sized DRG neurons. Furthermore, the staining disappeared almost completely in NT-4 null mutant mice reflecting the loss of D-hair receptors. With this evidence, we can conclude that we identified the first gene in the DRG that is specifically expressed in D-hair mechanoreceptors. The logical question was whether this calcium channel plays a crucial role in D-hair mechanoreceptor function and whether D-hair receptor function can be inactivated by blocking the calcium channel. There are two relatively selective antagonists of this group of T-type calcium channels known, mibefradil and nickel.

The tetralol derivative mibefradil is a calcium channel antagonist, structurally and functionally different from the dihydropyridine L-type calcium channel blockers, with relative selectivity for T-type calcium channels. This drug was used as medication against hypertension and angina pectoris, but was retracted due to fatal interactions with other calcium channel blockers. It has an EC50 of ~1 μM on recombinant channels (Martin et al., 2000) and is equally effective on all three isotypes. In higher concentrations (10 times higher), it is also effective on the other voltage gated calcium channels. The EC50 of nickel on CaV3.2 is ~ 15 μM on recombinant channels, and it is more than 20 fold less effective on the CaV3.1 and CaV3.3 subtypes. Nickel is also a channel pore blocker (Lee et al, 1999, b). Although its relative selectivity for CaV3.2 made nickel a preferable antagonist for our studies, we chose mibefradil for our blocking experiments because nickel is also highly cytotoxic.

The EC50 of mibefradil is 1 μM on recombinant channels in patch clamp experiments and we assumed that we needed higher concentration in the skin nerve preparation. We found that bath

concentrations of 50 µM mibefradil had a dramatic blocking effect on the overall mechanotransduction (data not shown). This effect was not restricted to D-hair receptors, and we hypothesize that other voltage dependent calcium channels like L-type or N-type calcium channels, which are also blocked by these doses of mibefradil (Bezprozvanny and Tsien, 1995) may be expressed in other fiber types and have a still unknown function in mechanotransduction. Although this was a very interesting finding, we did not follow this up further and focused on the examination of D-hair mechanoreceptors.

In the next step, we quantitatively tested the effect of mibefradil on mechanical sensitivity. In this test, we isolated the receptive field of D-hair mechanoreceptors or AM high threshold mechanoreceptors respectively with a metal ring and applied mibefradil into the ring. Using a mechanical stimulator we applied repetitive mechanical stimuli onto the receptive field and responding action potentials were recorded. In order to achieve a more specific effect we decreased the mibefradil dose to 15 µm in the isolation ring. The EC50 on recombinant channels is about 1 µM, but we assumed that the ring application requires some compensation for dilution and diffusion effects.

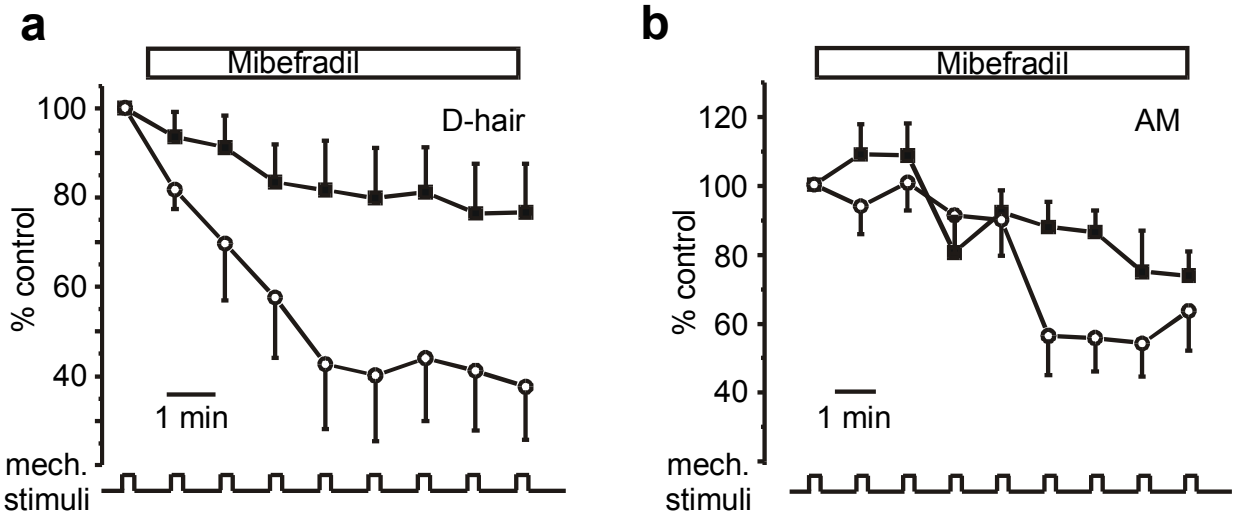

Figure 25: test for mechanical sensitivity in D-hair and AM mechanoreceptors. A repetitive mechanical stimulus of 150 µm was applied to D-hair and AM receptors in the presence or absence of 15 µM mibefradil (n=8-9 fibers per group). Open circles represent mibefradil treated, black squares are control buffer treated units. The response of the units in panel a is normalized to the value prior to mibefradil or control buffer application. The D-hair receptors show a small decrease in response over time in the absence of mibefradil, however in the presence of the drug response amplitude was further decreased to 40% of control values ($p<0.05$, repeated measures ANOVA). AM fibers were subjected to the same

procedure in panel b and units treated with mibefradil showed no significant reduction of response amplitude after drug application (p>0.40 repeated measure ANOVA n=8-9 units per group).

The control curve for D-hair receptors shows a slight decrease of response with time. Mibefradil application decreases the sensitivity of D-hair receptors to around 40 % of the buffer control. In AM fibers, there was no significant difference in the response of neurons treated with buffer or mibefradil.

Next we wanted to test, whether the mechanical threshold of D-hair and AM mechanoreceptors was affected. The common way to determine the mechanical threshold is to use calibrated v. Frey monofilaments (Frey M, 1897). The minimal force that can be applied using v. Frey monofilaments is 0,4 mN, and this is above the threshold for D-hairs which was determined in in vivo experiments (Lewin et al., 1992). Therefore we decided to measure the mechanical threshold indirectly by measuring the latency. We applied a ramp form mechanical indentation to the skin using a mechanical stimulator with a constant forward driving velocity. If we measure the time from the beginning of the mechanical stimulus to the first responding action potential, this time latency is directly proportional to the indentation that was needed to evoke the first action potential.

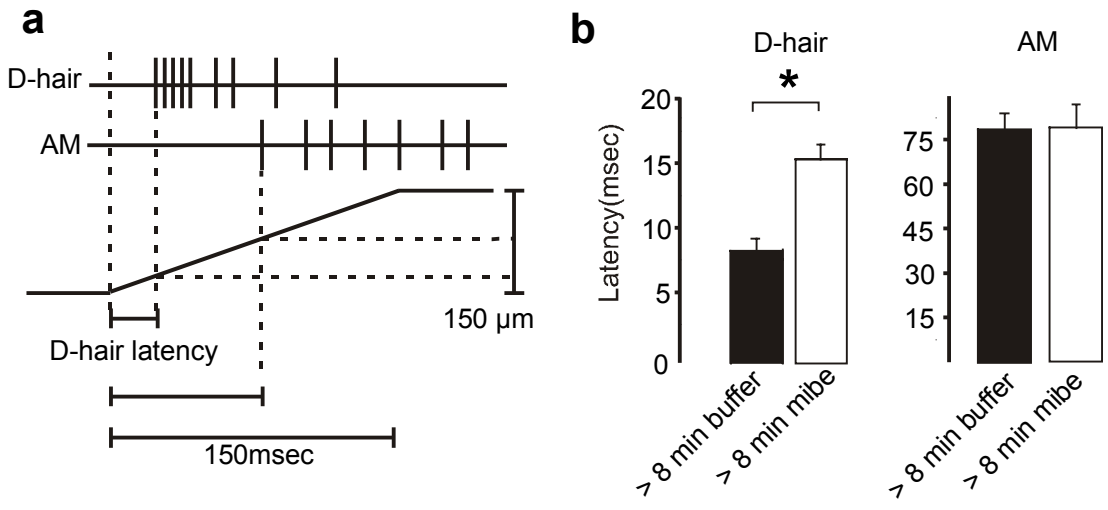

Figure 26: a) illustrates the linear relationship between latency and skin indentation. b) mechanical latencies of D-hair and AM mechanoreceptors after mibefradil treatment. D-hair receptors have short mechanical latency (~ 8 msec) whereas AM high threshold mechanoreceptors have longer latencies (~80 msec). Mechanical latency of D-hair receptors increases significantly in mibefradil compared to buffer (45% increase) (p<0.01,

ANOVA). No significant effect of mibefradil treatment on AM mechanical latency was observed.

In D-hair receptors we observed a significant increase of latency after mibefradil treatment, whereas no change was observed in AM nociceptive receptors.

In the next experiment we examined whether the effect on mechanosensitivity was due to decreased excitability of the receptor. We therefore decided to measure spike frequency adaptation, a technique whereby a microelectrode is used to deliver trains of suprathreshold electrical stimuli of increasing frequency to the receptor ending. This method allowed us to examine the ability of the receptor to follow electrical stimulation at different frequencies and is an indirect test of the fibers electrical excitability.

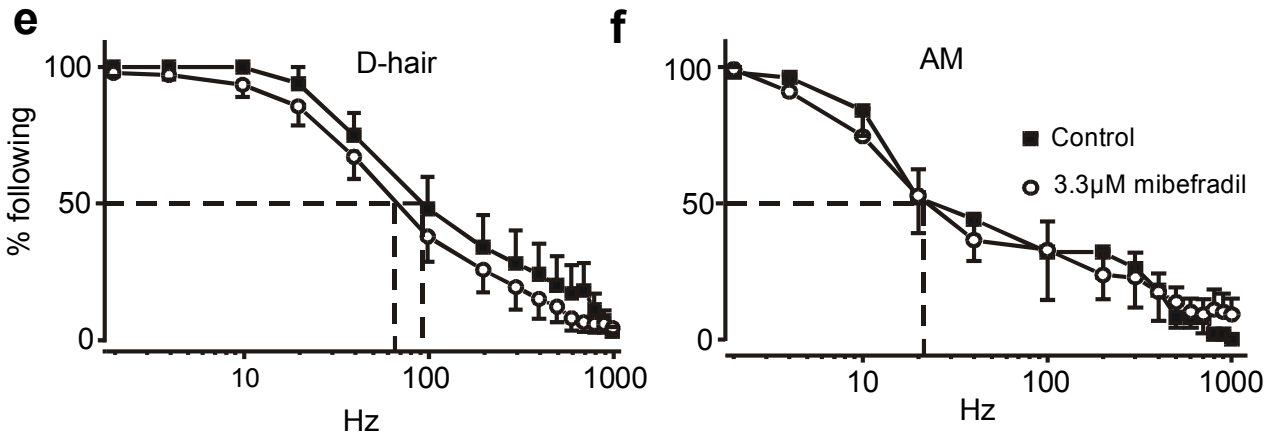

Figure 27: Measurements of spike frequency adaptation in a large sample of D-hair and AM receptors is shown (n=20-36 units per group). Plots in of mibefradil (3.3µM) treated fibers (open circles) and control untreated fibers (closed squares). The percentage of stimuli in which the unit discharged one spike per stimulus is plotted as a function of the stimulus frequency (10 stimuli per frequency). The spike frequency adaptation curve for D-hair receptors is shifted leftward in the presence of mibefradil whereas no change was observed in AM receptors.

At low frequencies (< 10 Hz) an action potential follows each electrical stimulus in both D-hair and AM receptors. As the frequency is increased, the percentage of failures steadily increases. When a large number of such recordings were made, it became clear that AM-fibers were less able to follow high frequency trains than are D-hair receptors. The median following frequency

for the sample of AM fibers was just over 20 Hz compared to 100 Hz for D-hair receptors. In the presence of just 3.3 μM of mibefradil (near the EC50 for mibefradil measured on recombinant channels (Martin et al. ,2000) a leftward shift in spike frequency adaptation was observed for D-hair receptor, median frequency 40 Hz, but no change was seen for AM fibers. Together, this data indicate that both the mechanical and electrical excitability of D-hair receptor endings is selectively reduced during T-type calcium channel blockade. Thus the selective expression of the CaV3.2 channel subunit in D-hair receptors demonstrated here might contribute to the unique sensitivity of these receptors.

The skin-nerve preparation experiments were carried out together with Carlos Martinez Salgado.